SUPPORTING INFORMATION

In Vivo Evaluation of Multifunctional Gold Nanorods for Boron Neutron Capture and Photothermal Therapies

Krishna R. Pulagam,[a] Malou Henriksen-Lacey,[a,b] Kepa B. Uribe,[a] Carlos Renero-Lecuna,[a] Jatish Kumar,[c] Alexandra Charalampopoulou,[d] Angelica Facoetti,[d] Nicoletta Protti,[e,f] Vanessa Gómez-Vallejo,[a] Zuriñe Baz,[a] Vished Kumar,[a] Ana Sánchez-Iglesias,[a,b] Saverio Altieri,[e,f] Unai Cossío,[a] Desire Di Silvio,[a] Angel M. Martínez-Villacorta,[a] Ane Ruiz de Angulo,[g] Luka Rejc,[a,h] Luis M. Liz-Marzán,[a,b,i] and Jordi Llop[a,j]*

[a] CIC biomaGUNE, Basque Research and Technology Alliance (BRTA), Paseo de Miramón 194, 20014 Donostia-San Sebastian, Spain.

[b] Centro de Investigación Biomédica en Red de Bioingeniería, Biomateriales y Nanomedicina (CIBER-BBN), Paseo de Miramón 194, 20014 Donostia-San Sebastian, Spain

[c] Department of Chemistry, Indian Institute of Science Education and Research (IISER) Tirupati, Tirupati 517507, India.

[d] Research and Development Department, CNAO National Center for Oncological Hadrontherapy, Pavia, Italy.

[e] Department of Physics, University of Pavia, 27100 Pavia, Italy.

[f] National Institute of Nuclear Physics, Pavia Section, 27100 Pavia, Italy.

[g] CIC bioGUNE, Basque Research and Technology Alliance (BRTA), Bizkaia Science & Technology Park bld 801 A, 48160 Derio, Bizkaia, Spain.

[h] University of Ljubljana, Faculty of Chemistry and Chemical Technology, Večna pot 113, Ljubljana, Slovenia.

[i] Ikerbasque, Basque Foundation for Science, 48013 Bilbao, Spain.

[j] Centro de Investigación Biomédica en Red de Enfermedades Respiratorias (CIBERES), 28029 Madrid, Spain.

[*] e-mail: jllop@cicbiomagune.es; Phone number: +34 943 005 333

Evaluation of the number of reactions per second on ^{10}B and ^{197}Au by thermal neutrons

Consider a mass m_{Au} exposed to a thermal neutron flux Φ ($cm^{-2}s^{-1}$). The number of reactions per second (R_{Au}) that occur during the neutron irradiation is given by:

$$R_{Au} = \frac{m_{Au}}{A_{Au}} N_A \sigma_{Au} \emptyset$$

where A_{Au} is the mass number of Au, N_A is the Avogadro number and σ_{Au} the capture cross section for thermal neutron of ^{197}Au(n,γ)^{198}Au reaction.

Similarly, for a mass m_B of ^{10}B exposed to the same flux of thermal neutrons the number of reactions per second R_B is given by:

$$R_B = \frac{m_B}{A_B} N_A \sigma_B \emptyset$$

where A_B is the mass number of ^{10}B, and σ_B the capture cross section for thermal neutron of ^{10}B(n,α)^{7}Li reaction on which the BNCT is based.

Therefore, the ratio between the number of reactions per second between ^{10}B and ^{197}Au is given by:

$$\frac{R_B}{R_{Au}} = \frac{m_B}{m_{Au}} \frac{A_{Au}}{A_B} \frac{\sigma_B}{\sigma_{Au}} = \frac{m_B}{m_{Au}} \frac{197}{10} \frac{3840}{98.8} = \frac{m_B}{m_{Au}} \, 765.7$$

For AuNRs we have $\frac{m_B}{m_{Au}} = 0.1$

If the Boron used in AuNRs is a 100% ^{10}B enriched:

$$\frac{R_B}{R_{Au}} = \frac{m_B}{m_{Au}} \, 765.7 = 0.1 \cdot 765.7 = 76.57$$

If natural Boron (20% ^{10}B and 80% ^{11}B) is used in GNR, then:

$$\frac{R_B}{R_{Au}} = \frac{m_B}{m_{Au}} \, 765.7 = 0.1 \cdot 0.2 \cdot 765.7 = 15.3$$

The previous numbers confirm that considering the gold/boron composition of our nanosystems, and assuming natural abundance of ^{10}B (20%), for every 15 reactions on

^{10}B there is only one reaction on the ^{197}Au; in the case of a 100% abundance of ^{10}B (as used in BNCT) there is one reaction on ^{197}Au every about 77 reactions on ^{10}B.

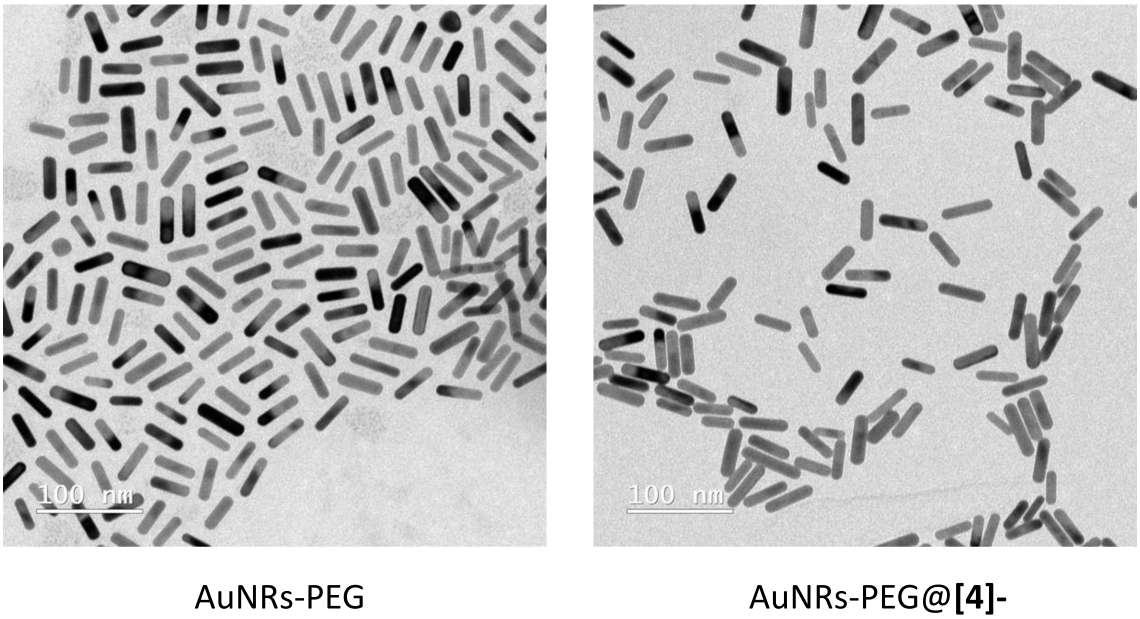

Figure S1. Representative TEM micrographs of AuNRs-mPEG (left) and AuNR-mPEG@**[4]**$^-$ (right), prior to laser irradiation.

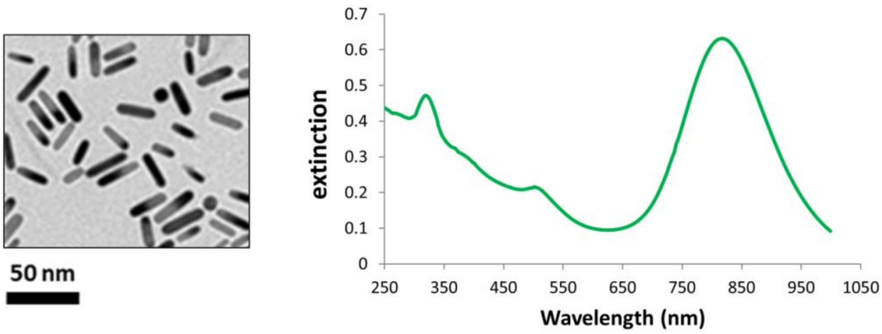

Figure S2. Left: Representative transmission electron micrograph (TEM) of [^{64}Cu]AuNR-mPEG@**[4]**$^-$. Right: UV-Vis-NIR extinction spectrum of [^{64}Cu]AuNR-mPEG@**[4]**$^-$. Both characterizations were performed after complete radioactive decay.

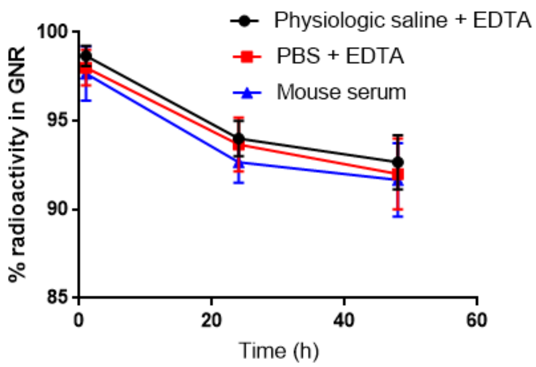

Figure S3. Radiochemical stability of AuNR-mPEG@**[4]**$^-$ at different incubation times in 0.9% NaCl + 2.5 mM EDTA, 10 mM PBS + 2.5 mM EDTA, and mouse serum.

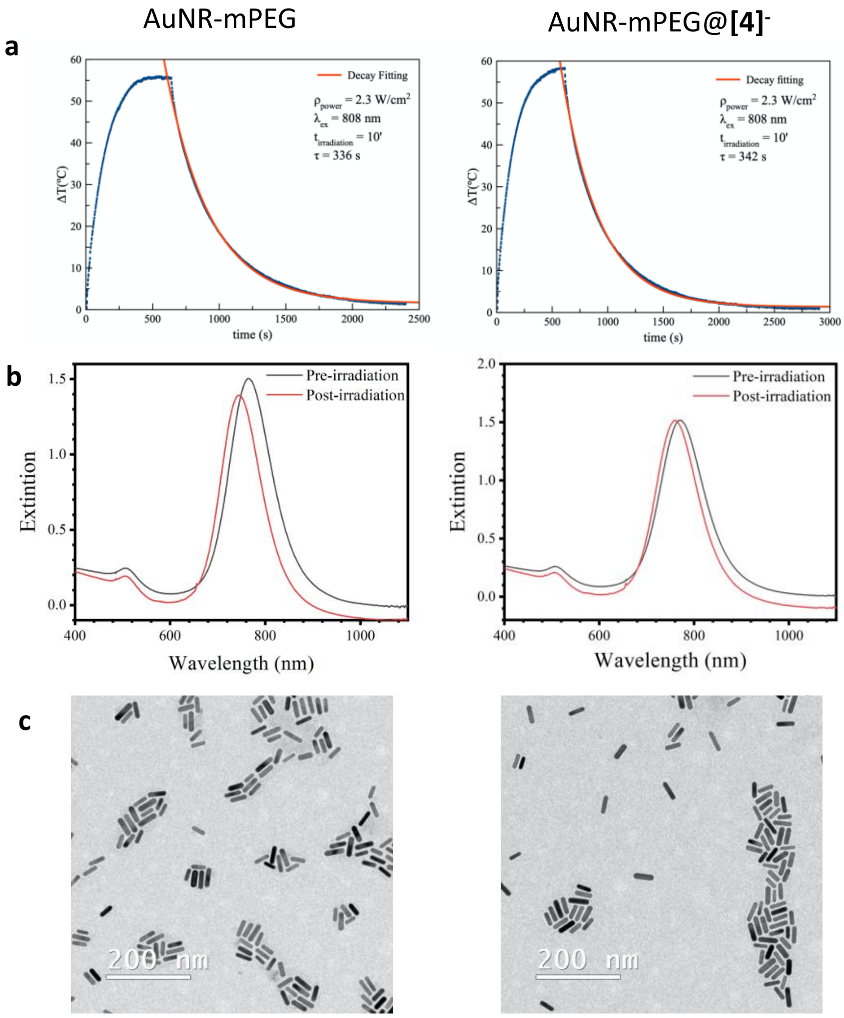

Figure S4. Effect of laser irradiation on AuNR-mPEG and AuNR-mPEG@**[4]**$^-$ ([Au] = 20 µg/mL, laser power = 2.3 W/cm^2). Photothermal characterization (a), UV-Vis spectra (b), and representative TEM micrographs (c), obtained before (left column) and after (right column) laser irradiation. A slight decrease in aspect ratio is observed post irradiation, correlating to a slight LSPR blue shift of 20 nm and 11 nm for AuNR-mPEG and AuNR-mPEG@**[4]**$^-$ AuNRs, respectively.

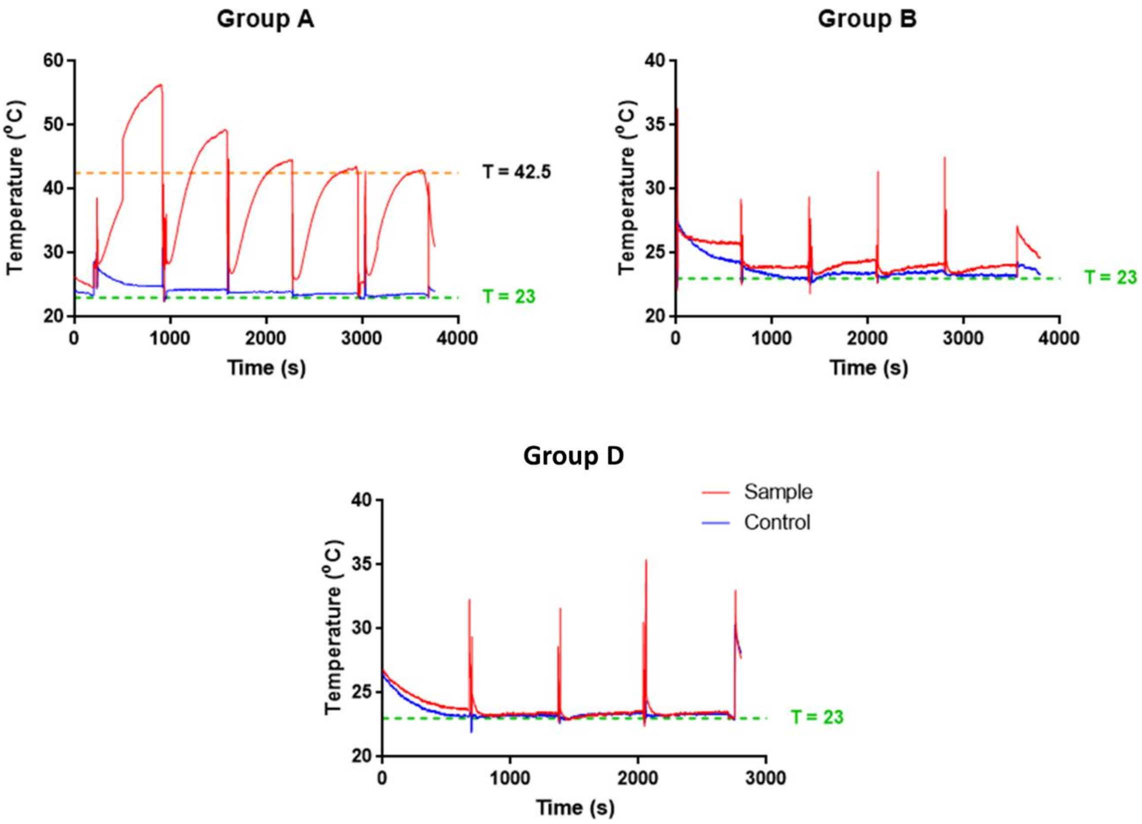

Figure S5. Temperature curves of the irradiated wells for groups A-C. Red curves represent temperature profiles of wells containing the spheroids; blue lines represent temperature profiles of adjacent empty wells; Group A: spheroids incubated with AuNRs (concentration = 20 µg/mL in gold) followed by NIR irradiation; B: spheroids incubated with AuNRs followed by media exchange and NIR irradiation; Group D, spheroids incubated in the absence of AuNRs and subjected to laser irradiation.

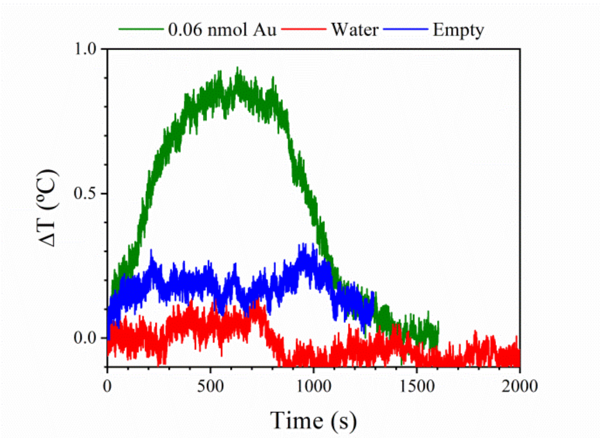

Figure S6. Temperature curves obtained during NIR irradiation of an aqueous solution containing AuNR-mPEG@**[4]**$^{-}$ at a concentration of 64 pmol/100 µL (green line). Red and blue curves represent temperature profiles of wells containing water and air, respectively.